JOURNAL OF COMPUTATIONAL PHYSICS 46, 54–68 (1982)

Elliptic-Vortex Method for Incompressible Flow at High Reynolds Number*

ZHEN-HUAN TENG

Department of Mathematics, Peking University, Peking, China
and Department of Mathematics, University of California, Berkeley, California 94720

Received July 30, 1981

An elliptic-vortex model for approximating the time-dependent Navier–Stokes equations at high Reynolds number is presented. One attractive feature of the new method is that the elliptic-computational elements used in this model are very good for boundary layer flow. Also introduced are a modified boundary algorithm and a new outflow boundary condition. Numerical computations for flat-plate problems show that the new method converges very fast and the numerical results are in excellent agreement with known facts.

1. INTRODUCTION

The random-vortex method published by Chorin in [4] is a grid-free method. This method is suitable for analysis of flow at high Reynolds number because it has no obvious intrinsic source of diffusion. The features of this method are as follows: the inviscid parts of the equation are taken into account by analysis of the interactions between vortices of small but finite core ("vortex blob"); viscous diffusion is taken into account by adding to the motion of vortices a Gaussian random component of appropriate variance, and the no-slip boundary conditions are approximated by a vorticity-creation procedure.

There are some difficulties with this method, however. Mainly, its convergence is slow near the boundary (see Chorin *et al.* [7]) and the results are not always independent of numerical parameters (see Ashurst [1]). To overcome this problem, Choring published in [5] the vortex-sheet method. Vortex-sheet elements could be used near the boundary, at the cost of replacing the Navier–Stokes equations by the Prandtl boundary-layer equations. So the important boundary-layer instability cannot be seen in the sheet method. For solving this problem, Chorin [6] used a hybrid method resulting from a coupling of the vortex-sheet method at the inner flow and the vortex-blob method at the outer flow to calculate physical instability. Also Cheer did

* This work was supported in part by the Director, Office of Energy Research, Office of Basic Energy Sciences, Engineering, Mathematical, and Geosciences Division of the U. S. Department of Energy under Contract W-7404-ENG-48.

0021-9991/82/040054–15$02.00/0

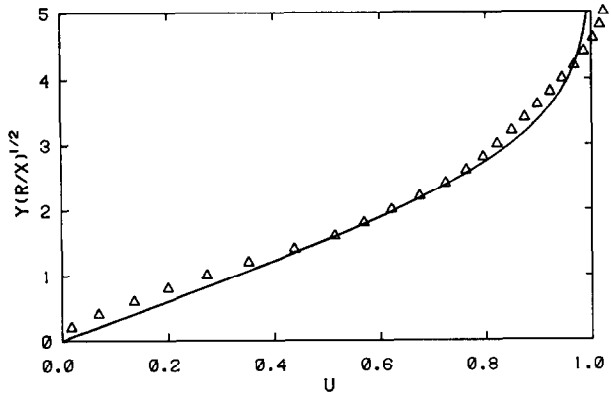

FIG. 1. Average velocity between $t = 4$ and $t = 6$ for $R = 2 \times 10^3$ (△) and Blasius profile (—).

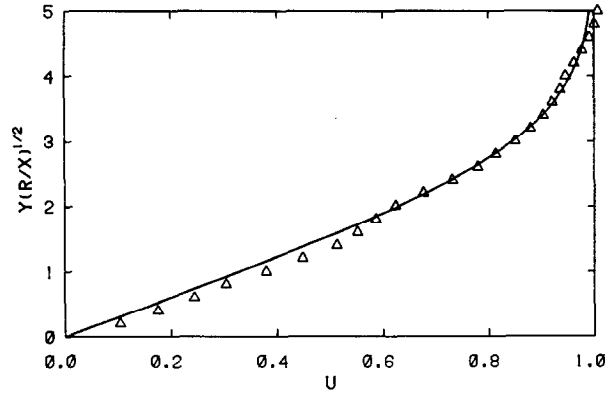

FIG. 2. Average velocity between $t = 4$ and $t = 6$ for $R = 5 \times 10^3$ (△) and Blasius profile (—).

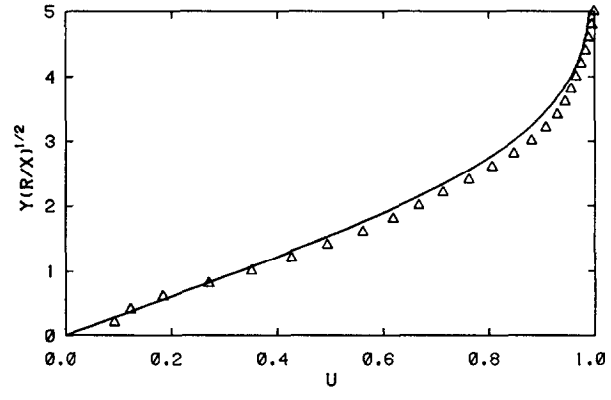

FIG. 3. Average velocity between $t = 4$ and $t = 6$ for $R = 10^4$ (△) and Blasius profile (—).

this for flow past a circular cylinder in [3]. Obviously, transition from sheets to blobs involves a decision process which is not unambiguous.

In this paper we shall present an elliptic-vortex model which can overcome all the difficulties above. The main merits of the new model are as follows:

(i) This method converges fast near the boundary because the elliptic structure of the vortex is suitble for boundary flow.

(ii) The elliptic-vortex method solves the Navier–Stokes equations and, thus, it is useful both for the inner flow and for the outer flow.

(iii) The cutoff length, i.e., the lengths of the major and the minor axis of the elliptic-computational elements, can be determined in a natural way, and as a result the numerical results obtained are independent of numerical parameters.

We shall also introduce a modified boundary algorithm. In this algorithm, a vortex that hits the boundary bounces from the boundary for the inviscid part of the flow, and diffuses through the boundary for the viscous part of the flow. We also give a new outflow-boundary condition which makes the calculation stable and accurate.

Numerical calculations are carried out for the semi-infinite flat-plate problem. In the test calculations we use a rather large step and space step. The results agree quite well with known facts. For example, the average horizontal velocities over 10 time steps between $t = 4$ and $t = 6$ at $R = 2 \times 10^3$, $R = 5 \times 10^3$, and $R = 10^4$ are in excellent agreement with the laminar steady Blasius profile (see Fig. 1, Fig. 2, and Fig. 3), and at $R = 10^5$ the average velocity over the same period of time exhibits a physical instability (see Fig. 5).

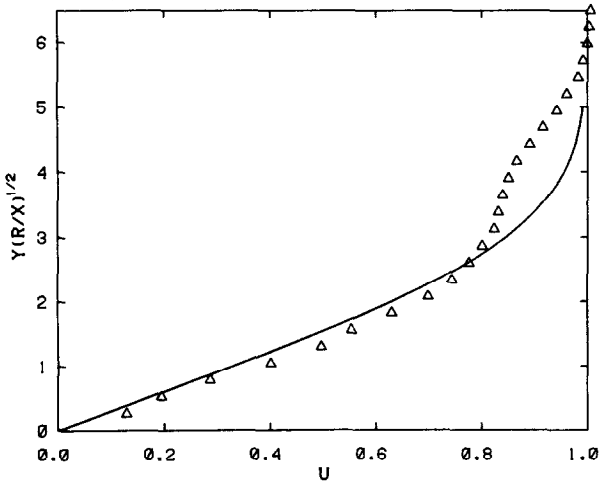

FIG. 4. Average velocity between $t = 4$ and $t = 6$ for $R = 5 \times 10^4$ (△) and Blasius profile (—).

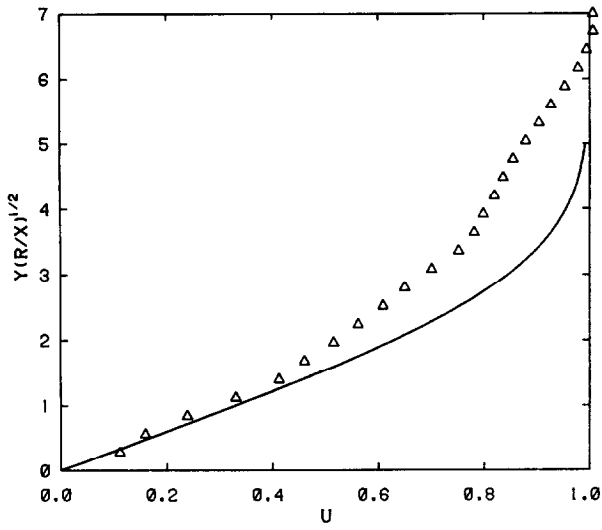

FIG. 5. Average velocity between $t = 4$ and $t = 6$ for $R = 10^5$ (△) and Blasius profile (—).

2. Elliptic-Vortex Blob Model in Two Dimensions

The Navier–Stokes equations for an incompressible flow can be written as

$$\begin{aligned} \partial_t \xi + (\mathbf{u} \cdot \nabla)\xi &= R^{-1} \Delta \xi, \\ \Delta \psi &= -\xi, \\ u = \partial_y \psi, \qquad v &= -\partial_x \psi, \end{aligned} \tag{1}$$

where $\mathbf{u} = (u, v)$ is the velocity vector, $\mathbf{r} = (x, y)$ is the position vector, t is the time, ψ is the stream function, $\xi = \partial_x v - \partial_y u$ is the vorticity, $\Delta \equiv \nabla^2$ is the Laplace operator and R is the Reynolds number.

First, we consider the inviscid, incompressible flow without boundaries. In this case, the Navier–Stokes equations above reduce to

$$\partial_t \xi + u \partial_x \xi + v \partial_y \xi = 0, \tag{2a}$$

$$\Delta \psi = -\xi, \tag{2b}$$

$$u = \partial_y \psi, \qquad v = -\partial_x \psi. \tag{2c}$$

For solving Eqs. (2), suppose the vorticity field ξ is now represented by the sum of vortices ξ_i with finite cores

$$\xi(x, y, t) = \sum_{i=1}^{N} \xi_i(x, y, t). \tag{3}$$

We shall suppose the vortices ξ_i are elliptic-vortex blobs, i.e., the vortices have finite-elliptic cores. The elliptic vortices ξ_i are defined by

$$\xi_i(x, y, t) = \Gamma_i \gamma(x - x_i(t), y - y_i(t)), \tag{4}$$

where Γ_i are their respective circulations, $(x_i(t), y_i(t))$ are the present locations of the vortices, and γ is a uniform vorticity distribution over an ellipse $\Omega(a, b)$. The γ is given by

$$\begin{aligned} \gamma(x, y) &= 1/\sigma \qquad (x, y) \in \Omega(a, b), \\ &= 0 \qquad (x, y) \bar{\in} \Omega(a, b), \end{aligned} \tag{5}$$

where $\Omega(a, b)$ is an ellipse with major axis a and minor axis b, defined by

$$\Omega(a, b) = \{(x, y) \mid (x^2/a^2) + (y^2/b^2) \leqslant 1\}, \tag{6}$$

and

$$\sigma = \pi ab \tag{7}$$

is the area of $\Omega(a, b)$. Note that here the distribution γ or the elliptic shape $\Omega(a, b)$ is common to all vortex blobs ξ_i.

With assumptions (3) and (4), the stream function ψ will have the form

$$\psi = \sum_{i=1}^{N} \psi_i = \sum_{i=1}^{N} \Gamma_i \phi(x - x_i(t), y - y_i(t)) \tag{8}$$

with

$$\begin{aligned} \nabla^2 \phi(x, y) &= -1/\sigma \qquad (x, y) \in \Omega(a, b), \\ &= 0 \qquad (x, y) \bar{\in} \Omega(a, b). \end{aligned} \tag{9}$$

When $a = b$, the elliptic vortex blob ξ_i reduces to the circular-vortex blob (for this kind of model, see Chorin [4], Hald [9], and Leonard [12]). In the general case, a solution of the Eq. (9) can be expressed by a potential integral over the ellipse $\Omega(a, b)$

$$\phi(x, y) = \frac{1}{2\pi\sigma} \iint_{\Omega(a,b)} \ln \frac{1}{\sqrt{(x - \xi)^2 + (y - \eta)^2}} \, d\xi \, d\eta. \tag{10}$$

In fact (10) can be integrated out in closed form, but the process of calculation is rather cumbersome. Here we shall only give the results

$$\begin{aligned} \phi(x, y) &= \frac{-1}{2\pi(a + b)} \left(\frac{x^2}{a} + \frac{y^2}{b} \right) \qquad (x, y) \in \Omega(a, b), \\ &= \frac{-1}{2\pi} \left(\frac{(x^2/\alpha) + (y^2/\beta)}{\alpha + \beta} + \ln \frac{\alpha + \beta}{a + b} \right) \qquad (x, y) \bar{\in} \Omega(a, b), \end{aligned} \tag{11}$$

where

$$\alpha = \sqrt{a^2 + \lambda}, \qquad \beta = \sqrt{b^2 + \lambda} \tag{12}$$

and λ (>0) satisfies

$$x^2/(a^2 + \lambda) + y^2/(b^2 + \lambda) = 1. \tag{13}$$

It is easy to verify that function (11) is continuously differentiable in the whole space and satisfies the Eq. (9). With formula (11) in hand, we can find the induced velocity field by taking the derivative of the stream function (8). Thus

$$\begin{aligned} u(x, y, t) &= \sum_{i=1}^{N} \Gamma_i \, \partial_y \phi(x - x_i(t), y - y_i(t)), \\ v(x, y, t) &= -\sum_{i=1}^{N} \Gamma_i \, \partial_x \phi(x - x_i(t), y - y_i(t)). \end{aligned} \tag{14}$$

By some calculations on (11) one gets

$$\begin{aligned} \partial_y \phi(x, y) &= \frac{-1}{\pi(a+b)} \frac{y}{b} \qquad (x, y) \in \Omega(a, b), \\ &= \frac{-1}{\pi(\alpha+\beta)} \frac{y}{\beta} \qquad (x, y) \bar{\in} \Omega(a, b), \end{aligned} \tag{15}$$

and

$$\begin{aligned} \partial_x \phi(x, y) &= \frac{-1}{\pi(a+b)} \frac{x}{a} \qquad (x, y) \in \Omega(a, b), \\ &= \frac{-1}{\pi(\alpha+\beta)} \frac{x}{\alpha} \qquad (x, y) \bar{\in} \Omega(a, b), \end{aligned} \tag{16}$$

where α, β are defined by (12) and (13).

According to the inviscid vorticity-transport equation (2a), the motion of the vortex blobs is described by the induced velocity field at its present position

$$\frac{dx_i(t)}{dt} = u(x_i(t), y_i(t), t), \qquad \frac{dy_i(t)}{dt} = v(x_i(t), y_i(t), t), \tag{17}$$

where the induced velocity u, v are given by (14). For simplicity Eqs. (17) are approximated by Euler's method

$$\tilde{x}_i^{n+1} = x_i^n + u(x_i^n, y_i^n, nk)k, \qquad \tilde{y}_i^{n+1} = y_i^n + u(x_i^n, y_i^n, nk)k, \tag{18}$$

where k is a time step, $x_i^n = x_i(nk)$ and $y_i^n = y_i(nk)$ are the coordinates of the vortex ξ_i.

Next we shall consider the diffusion part of the Navier–Stokes equations,

$$\partial_t \xi = R^{-1} \nabla^2 \xi. \tag{19}$$

The heat equation is well known to be solvable by a random-walk algorithm (see Chorin [4]). As a result, Eq. (19) can be solved by moving the blobs according to the law

$$x_i^{n+1} = \tilde{x}_i^{n+1} + \eta_1, \qquad y_i^{n+1} = \tilde{y}_i^{n+1} + \eta_2, \tag{20}$$

where η_1, η_2 are independent Gaussian-random variables with mean zero and variance $2k/R$.

In summary, the procedure for approximating Eqs. (1) is as follows: the vortex blobs are moved by the laws (18), (20), and then the new velocity field (14) is determined by the vortex blobs at their new positions.

Note that in the vortex method we use clouds of nondeformable, nonrotational numerical-vortex elements to approximate the motion of deformable physical vortices. The collective motion resolves all effects, including the rotation and deformation effects. The convergence theories of the vortex-blob method to the solution of the Euler equations (see Hald [9] and Beale and Majda [2]) and partial convergence results for Navier–Stokes equations (see Chorin *et al.* [7]) lend support to this expectation.

3. Symmetry Extension and Vortex Generation

We shall consider incompressible flow with boundaries. In the following we shall only dicuss flow past a semi-infinite flat plate.

Suppose a semi-infinite flat plate is placed on the positive half-axis in an incompressible fluid of density 1 occupying the half space $y \geqslant 0$. At time $t < 0$ the fluid is at rest. At $t = 0$, the fluid is impulsively set into motion with velocity U_∞. The flow is described by the Navier–Stokes equation (1) with the boundary conditions

$$\mathbf{u} = (U_\infty, 0) \qquad \text{at} \quad y = \infty, \quad t > 0 \tag{21a}$$

$$u = v = 0 \qquad \text{at} \quad y = 0, \quad x > 0 \tag{21b}$$

$$\frac{\partial v}{\partial y} = 0 \qquad \text{at} \quad y = 0, \quad x < 0. \tag{21c}$$

Initially $\mathbf{u} = (U_\infty, 0)$, everywhere.

The vortex-blob method described in the previous section approximates the Navier–Stokes equations (1) without boundary (21). Suppose at some moment $t = nk$ there are N vortex blobs $\zeta_i(x, y, t)$ at the upper space ($y > 0$). Generally, the flow induced by the vortices does not satisfy the boundary conditions (21). To satisfy the zero normal-velocity condition $v = 0$, the image method will do the job. The image

method is as following: for each elliptic-vortex blob $\xi_i(x, y, t) = \Gamma_i \gamma(x - x_i, y - y_i)$ with $y_i > 0$, we set its image-vortex blob

$$\bar{\xi}_i(x, y, t) = -\Gamma_i \gamma(x - x_i, y + y_i) \tag{22}$$

at the symmetric point $(x_i, -y_i)$ of the lower space.

Using a procedure similar to the one in Section 2, we know that the vortices ξ_i $(i = 1,..., N)$, together with their image vortices $\bar{\xi}_i$ $(i = 1,..., N)$, define the stream function as

$$\psi(x, y, t) = \sum_{i=1}^{N} \Gamma_i(\phi(x - x_i, y - y_i) - \phi(x - x_i, y + y_i)) \tag{23}$$

and, thus, the induced velocity as

$$\begin{aligned} u(x, y, t) &= \sum_{i=1}^{N} \Gamma_i(\partial_y \phi(x - x_i, y - y_i) - \partial_y \phi(x - x_i, y + y_i)), \\ v(x, y, t) &= -\sum_{i=1}^{N} \Gamma_i(\partial_x \phi(x - x_i, y - y_i) - \partial_x \phi(x - x_i, y + y_i)). \end{aligned} \tag{24}$$

From this we can see that the induced velocity field is symmetric with respect to the boundary $y = 0$:

$$\begin{aligned} u(x, y, t) &= u(x, -y, t) \\ v(x, y, t) &= -v(x, -y, t) \end{aligned} \tag{25}$$

and its normal velocity v at the wall $(y = 0)$ equals zero

$$v(x, 0, t) = 0. \tag{26}$$

This tells us that the image method continues the flow from the upper space to the lower space by a symmetric extension (25). As a result

$$\xi(x, y) = -\frac{\partial u(x, y)}{\partial y} + \frac{\partial v(x, y)}{\partial x} = \frac{\partial u(x, -y)}{\partial y} - \frac{\partial v(x, -y)}{\partial x} = -\xi(x, -y).$$

Note that since we are not assuming that ξ is continuous in the flow consisting of the real flow and its image, the condition above does not imply $\xi(x, 0) \equiv \lim_{y \to +0} \xi(x, y) = 0$.

Here we point out that for Prandtl equations there may have been another way of extending the flow to take care of the normal boundary condition. For example, in [5] Chorin used an antisymmetry $\mathbf{u}(x, -y) = -\mathbf{u}(x, y)$ to extend the velocity field

across the wall for the sheets method. Since $\xi = -\partial u/\partial y$ in the Prandtl-boundary equations, the antisymmetry leads to

$$\xi(x, y) = -\frac{\partial u(x, y)}{\partial y} = \frac{\partial u(x, -y)}{\partial y} = \xi(x, -y).$$

For the Navier–Stokes equations $\mathbf{u}(x, y) = -\mathbf{u}(x, -y)$ cannot lead to $\xi(x, y) = \xi(x, -y)$ and, thus, antisymmetry extension cannot be used here. As shown above the symmetry leads to $\xi(x, y) = -\xi(x, -y)$.

The remaining no-slip boundary condition $u = 0$ at $y = 0$ can be satisfied through the following vorticity-creation algorithm. Suppose the velocity component $u(x, 0, t)$, calculated by (24), is not equal to zero. The effect of viscosity will create a thin boundary layer just above the wall which will ensure a smooth transition from the boundary to the inside flow. As described by Chorin in [4], an array of vortices will approximate these features, and its induced velocity field will annihilate the tangential velocity $u(x, 0, t)$ at the boundary.

We now put this idea into practice for the elliptic-vortex model. First divide the boundary $\{(x, 0) \mid 0 \leqslant x \leqslant X\}$ into M segments of equal length h with centers Q_i, $i = 1,..., M$; let the coordinates of Q_i be $(X_i, 0)$ and the tangential velocity be $u(X_i, 0)$. At each point Q_i create $2l_i$ vortices ξ_j $(j = 1,..., 2l_i)$, with structure (4) and of equal intensive Γ_i, where l_i is an integer to be determined in the next section. In the following we shall discuss how to satisfy the tangent velocity by the new vortices and to determine the vortex parameters a, b, and Γ_i. The major axis a can be easily determined. Since we want to piece together the vortex elements created at different boundary points Q_i into a single vortex layer, so the length of the major axis ought to equal the distance between the neighboring points, i.e.,

$$a = h/2. \tag{27}$$

Another requirement is that the velocity field induced by the vortices ξ_j $(j = 1,..., 2l_i)$ at Q_i, must have an opposite sign velocity of $u(X_i, 0)$ at their lower vertex $(X_i, -b)$ and, thus, after random walk the newly created vortices located at the upper space with their image vortices can cancel the boundary velocity $u(X_i, 0)$. From this and (14), (15) we can determine the intensity Γ_i of the vortices as

$$\Gamma_i = -(\pi(a + b)/2l_i)\, u(X_i, 0). \tag{28}$$

Next, we shall let the vortices move by law (20). On the average, half of the vortices created at the boundary will walk into the upper space. At the same time the other half of the vortices will flow to the lower space, and cancel, at the boundary, with their image vortices. We know that after a random walk, if half of the new vortices ξ_j walk into the upper space with their lower vertices just on the boundary point Q_i, the induced velocity by the new vortices with their image vortices will exactly annihilate the $u(X_i, 0)$. Because of the random character, we cannot do it exactly. But we can make the mean coordinates of their lower vertices fall on the

boundary point Q_i, if we choose b equal to the mean distance of the random walk to the positive y axis, i.e.,

$$b = \frac{1}{\sqrt{\pi k/R}} \int_0^\infty y e^{-(y^2/4k)/R}\, dy = 2\sqrt{\frac{k}{\pi R}}. \tag{29}$$

According to the analysis above we can see that $b = 2\sqrt{k/\pi R}$ is the best choice for satisfying the boundary condition $u = 0$. So now all the parameters Γ_i, a, b have been determined. Here we have to point out that the major axis b, by (29), depends on both the time step k and the Reynolds number R. From (29) we know that the width of an elliptic-vortex blob, i.e., the minor axis $2b$, is of the same order of the boundary layer thickness $O(1/\sqrt{R})$. So we think this kind of elliptic-vortex blob is suited for mimicking the boundary flow.

To reduce the statistical error wa can require that the new blobs move by law (20) only along the y-axis direction and exactly half of them disappear at each step. The former requirement can be accomplished by choosing $\eta_1 = 0$ in (20). For the latter, a rejection technique [6] is used which ensures that successive η_2's used in (20) have opposite signs, and upon application of formula (20), exactly one half will flow to the upper space.

Using the algorithm described above we see that the normal boundary condition is satisfied exactly, but the tangential condition is satisfied statistically.

4. Vortex Bouncing, Diffusion at the Wall and Outflow-Boundary Condition

Here we shall present a special treatment of the boundaries. According to formula (26), we know that the vortex ξ_j cannot pass through the boundary ($y = 0$) due to the inviscid motion (17). But when we use the discrete formula (18), this may happen (i.e., $\tilde{y}_i^{n+1} < 0$). In our calculation, if the vortices cross the bundary we reflect them back into the fluid.

As for the viscous motion (20), the vortex ξ_i may cross the wall. By the symmetry of the fluid at $y = 0$, while a vortex ξ_i walks into the lower space its image vortex $\bar{\xi}_i$ will walk into the upper space. This suggests to us the following algortihm: If $y_i^{n+1} = \tilde{y}_i^{n+1} + \eta_1 < 0$, we set $\bar{\xi}_i = -\Gamma_i \gamma(x - x_i^{n+1}, y + y_i^{n+1})$ at $(x_i^{n+1}, -y_i^{n+1})$.

Finally, we discuss the outflow conditions. Because we have to restrict the size of the region, e.g., $0 \leqslant x \leqslant 1$, in which we do our computation, we need to impose a boundary condition at the outflow boundary $x = 1$. It is known that a bad outflow condition may cause oscillations of the velocity profile in the region of interest. Hedstrom and Ortenheld in [10] give a detailed discussion about this. They use a discrete form of the condition $uu_x = (1/R)u_{xx}$ and $v_y = -v_x$ at the outflow boundary. But there is no obvious way to put this kind of condition to work for the vortex method. Chorin in [6] gives an outflow condition which behaves as an absorbing boundary. He allows vortices to follow for $x > 1$, where detailed calculations are

performed at $0 \leqslant x \leqslant 1$, but to move only according to the random component in their law of motion. When they reach $x = 2$ they are deleted.

We shall give a modified algorithm. That is, when the vortex-blobs flow in the region $1 \leqslant x \leqslant 2$ we shall allow them to move not only with the random component but also with their own constant velocities in the motion (18), where the constant velocities are what they had when they just left the boundary $x = 1$. Our modified outflow condition looks like finite-plate outflow condition because there is no vortex generation at the piece of the wall $1 \leqslant x \leqslant 2$. Using the modified algorithm there, no oscillation occurs on the average velocity profile at $x = \frac{1}{2}$ (see Fig. 1–5).

5. Calculation Scheme

We shall give the detail of the algorithm and the formulas. First, discretize the boundary by dividing the boundary ($y = 0$, $0 \leqslant x \leqslant 1$) into M segments of equal length h with centers $Q_l = (X_l, 0)$ ($l = 1,..., M$). From the discussion in Section 3 we know that the ellipse $\Omega(a, b)$ is completely determined by

$$a = \frac{h}{2}, \qquad b = 2\sqrt{\frac{k}{\pi R}},$$

where k is a time step.

Suppose at some moment $t^n = nk$. There are $N(t^n)$ elliptic vortices ξ_l^n ($l = 1,..., N(t^n)$) at the upper space. By the formula (4), ξ_l^n can be determined by its position (x_l^n, y_l^n) and intensity Γ_l^n. So a computational element ξ_l^n can be expressed by $\xi_l^n = (\Gamma_l^n, x_l^n, y_l^n)$. The vortices ξ_l^n with their image vortices $\bar{\xi}_l^n = (-\Gamma_l^n, x_l^n, -y_l^n)$ induce a velocity field at $y \geqslant 0$

$$\begin{aligned} u^n(x, y) &= 1 + \sum_{j=1}^{N(t^n)} \Gamma_j^n(\partial_y\phi(x - x_j^n, y - y_j^n) - \partial_y\phi(x - x_j^n, y + y_j^n)), \\ v^n(x, y) &= -\sum_{j=1}^{N(t^n)} \Gamma_j^n(\partial_x\phi(x - x_j^n, y - y_j^n) - \partial_x\phi(x - x_j^n, y + y_j^n)). \end{aligned} \tag{30}$$

By substituting (15), (16) into (30) we obtain

$$\begin{aligned} u^n(x, y) &= 1 - \frac{1}{\pi(a+b)b}\left(\sum_1 \Gamma_j^n(y - y_j^n) - \sum_2 \Gamma_j^n(y + y_j^n)\right) \\ &\quad - \frac{1}{\pi}\left(\sum_3 \Gamma_j^n \frac{y - y_j^n}{(\alpha_j^n + \beta_j^n)\beta_j^n} - \sum_4 \Gamma_j^n \frac{y + y_j^n}{(\bar{\alpha}_j^n + \bar{\beta}_j^n)\bar{\beta}_j^n}\right) \\ v^n(x, y) &= \frac{1}{\pi(a+b)a}\left(\sum_1 \Gamma_j^n(x - x_j^n) - \sum_2 \Gamma_j^n(x - x_j^n)\right) \\ &\quad + \frac{1}{\pi}\left(\sum_3 \Gamma_j^n \frac{x - x_j^n}{(\alpha_j^n + \beta_j^n)\alpha_j^n} - \sum_4 \Gamma_j^n \frac{x - x_j^n}{(\bar{\alpha}_j^n + \bar{\beta}_j^n)\bar{\alpha}_j^n}\right), \end{aligned} \tag{31}$$

where

$$\alpha_j^n = \sqrt{a^2 + \lambda_j^n}, \qquad \beta_j^n = \sqrt{b^2 + \lambda_j^n}, \qquad \bar{\alpha}_j^n = \sqrt{a^2 + \bar{\lambda}_j^n}, \qquad \bar{\beta}_j^n = \sqrt{b^2 + \bar{\lambda}_j^n},$$

$\lambda_j^n\ (>0)$ satisfies $((x - x_j^n)^2/(a^2 + \lambda_j^n)) + ((y - y_j^n)^2/(b^2 + \lambda_j^n)) = 1,$

$\bar{\lambda}_j^n\ (>0)$ satisfies $((x - x_j^n)^2/(a^2 + \bar{\lambda}_j^n)) + ((y + y_j^n)^2/(b^2 + \bar{\lambda}_j^n)) = 1,$

$\sum_1$ is taken over all vortices ξ_j^n such that $(x - x_j^n, y - y_j^n) \in \Omega(a, b),$

$\sum_2$ is taken over all vortices $\bar{\xi}_j^n$ such that $(x - x_j^n, y + y_j^n) \in \Omega(a, b),$

$\sum_3$ is taken over all vortices ξ_j^n such that $(x - x_j^n, y - y_j^n) \bar{\in} \Omega(a, b),$

$\sum_4$ is taken over all vortices $\bar{\xi}_j^n$ such that $(x - x_j^n, y + y_j^n) \bar{\in} \Omega(a, b).$

For each time step k, the algorithm consists of two steps: First, at each boundary point Q_i, $2l_i$ vortices $\xi_j^n = (\Gamma_i, X_i, 0)$ $(j = 1,..., 2l_i)$, are generated, where

$$\begin{aligned} l_i &= 0, && \text{for } |u^n(X_i, 0)| \leqslant \tfrac{1}{2}u_{\max}, \\ &= [|u(X_i, 0)/u_{\max}|], && \text{for } |u^n(X_i, 0)| > \tfrac{1}{2}u_{\max}, \\ \Gamma_i &= -(\pi(a + b)/2l_i)\, u(X_i, 0) \end{aligned} \tag{32}$$

and $u_{\max}$ is some given small number. In (32), $|\cdot|$ means absolute value and $[\cdot]$ means the integer part of a real number.

The second step is to move the vortex blobs; the new vortices $\xi_j^n = (\Gamma_i, X_i, 0)(j = 1,..., 2l_i)$, move by the law

$$\begin{aligned} x_j^{n+1} = X_i, \qquad y_j^{n+1} = \eta_2, \qquad \Gamma_j^{n+1} &= \Gamma_i, && \text{for } y_j^{n+1} > 0, \\ &= 0, && \text{for } y_j^{n+1} \leqslant 0, \end{aligned}$$

where any two successive η_2's have different signs and thus only half of the new vortices move to the upper space. The old vortices $\xi_i^n = (\Gamma_i^n, x_i^n, y_i^n)$ with $y_i^n > 0$ move by

$$\begin{aligned} x_i^{n+1} &= x_i^n + \tilde{u}_i^n k + \eta_1, \\ y_i^{n+1} &= |\,|y_i^n + \tilde{v}_i^n k| + \eta_2|, \\ &= \Gamma_i^n, && \text{for } |y_i^n + \tilde{v}_i^n k| + \eta_2 > 0 \quad \text{and} \quad x_i^{n+1} < 2, \\ \Gamma_i^{n+1} &= -\Gamma_i^n, && \text{for } |y_i^n + \tilde{v}_i^n k| + \eta_2 < 0 \quad \text{and} \quad x_i^{n+1} < 2, \\ &= 0, && \text{for } x_i^{n+1} \geqslant 2, \end{aligned}$$

where

$$\begin{aligned} (\tilde{u}_i^n, \tilde{v}_i^n) &= (u^n(x_i^n, y_i^n), \quad v^n(x_i^n, y_i^n)) \quad \text{by (31), if} \quad x_i^n < 1 \\ &= (\tilde{u}_i^{n-1}, \tilde{v}_i^{n-1}), \qquad\qquad\qquad\qquad\qquad\qquad \text{if} \quad 1 \leqslant x_i^n \leqslant 2. \end{aligned}$$

After the two steps, $N(t^n)$ is changed by adding a number of newly created vortices located at the upper space and deducting the number of vortices which move out of the boundary $x = 2$, the new velocity (31) is determined by the vortices at their new positions and one goes back to the first part of the procedure. The procedure is started at $t = 0$ by setting $N(0) = 0$.

6. Numerical Results for a Semi-infinite Flat Plate

The physical problem of flow past a flat plate is described by the Navier–Stokes equations (1) and boundary conditions (21). For large Reynolds number R, the Prandtl-boundary layer equation (White [15], Chorin and Marsden [8]) should provide a reasonable description of the flow near the plate and away from the leading edge. The Prandtl equations have a stationary solution, the Blasius solution, which is a function of the similarity variable $\mu = y/\sqrt{xv}$, where $v = 1/R$ is the viscosity if $U_\infty = 1$ and $L = 1$. The Blasius solution is a very good test solution for Eqs. (1) and (21). It is known that the Blasius solution is unstable to infinitesimal perturbations which satisfy Eq. (1) (see Lin [13]) if $R_\delta = 1.72\sqrt{xR} \geqslant R_{\delta c}$; $R_{\delta c} \cong 520$ (see Jordinson [11]). For the perturbations of a finite amplitude the value of $R_{\delta c}$ given above has to be lowered. Since the vortex method will by its nature contain finite-amplitude perturbations, a substantial amount of noise and edge effect, the appropriate value of R_δ which separates stable fom unstable regimes is not clear. As described by Chorin in [6], there may exist a value $R'_{\delta c}$ such that for $R_\delta \leqslant R'_{\delta c}$ all perturbations decay. He suggests the best guess of $R'_{\delta c}$ is about 300, with a substantial margin of error. For $R_\delta \geqslant R'_{\delta c}$, presumably the erturbation grows and reaches some finite-amplitude equilibrium.

The numerical results obtained by our elliptic-vortex method agree quite well with the analysis given above. In our calculations, the boundary of the finite plate with length 1 is divided into $M = 5$ pieces, each of length $h = 1/M = 0.2$. The outflow condition is put on $1 \leqslant x \leqslant 2$. The time step is $k = 0.2$. The term $u_{\max} = 0.2$ is chosen. The Reynolds numbers R used are 2×10^3, 5×10^3, 10^4, 5×10^4, and 10^5 because at these ranges of R we can observe both physical stability and instability.

Figures 1–5 display the average velocities over 10 time steps between $t = 4.0$ and $t = 6.0$ as a function of $\mu = y/\sqrt{vx}$ at $x = 1/2$ for $R = 2 \times 20^3$, 5×10^3, 10^4, 5×10^4, and 10^5. To average the solution over a number of time steps (see [14]) can reduce the statistical error in the steady state. On the figures, (—) refers to the laminar steady Blasius profile, and (△) represent the numerical solutions of the horizontal velocity calulated by (31). From Figs. 1–3 we can see the numerical solutions are in very close agreement with the Balsius curves for $R = 2 \times 10^3$ ($R_\delta = 54$), $R = 5 \times 10^3$ ($R_\delta = 86$), and $R = 10^4$ ($R_\delta = 122$). Figure 4 displays some differences between the numerical solution and Blasius profile at large value of μ for $R = 5 \times 10^4$ ($R_\delta = 272$). It seems that the value $R_\delta = 272$ is the approximate value of $R'_{\delta c}$. In Figure 5 the numerical solution has more obvious departure from the Blasius profile at $R = 10^5$ ($R_\delta = 384$). That means for $R_\delta = 384$ ($> R'_{\delta c} = 300$) the perturbations of a finite

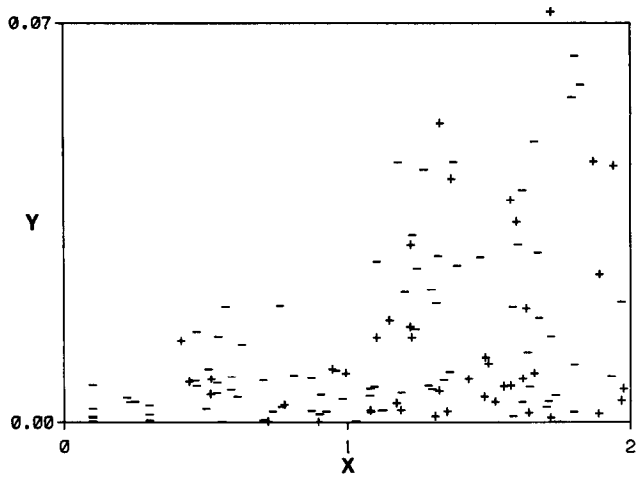

FIG. 6. Elliptic-vortex blobs over a flat plate.

amplitude can grow up. These results are reasonable in view of what is known from the theory and from experiment.

Comparing this with the hybrid method [6] and the circular-vortex method [1], we see that we could use a much bigger space step h and time step k and, furthermore, have results (Fig. 1–5) that look better. Why can the elliptic-vortex method get better results? The reason is that elliptic elements can induce an asymmetric-velocity field (15), (16). So we are able to adjust a and b (see (27) and (29)) to make the derivative of induced velocity along the direction tangent to the surface much smaller than the derivative in the normal direction. According to the boundary-layer theory this kind of elliptic blob is good for simulating boundary flow and thus fewer blobs are required to represent the boundary layer.

A typical run from $t=0$ to $t=6$ with the numerical parameters used here takes about 10 seconds on CDC 7600 computer at the Lawrence Berkeley Laboratory. At the end of the calculation there are about 50 blobs at $0 \leqslant x \leqslant 1$ and 80 blobs at $1 \leqslant x \leqslant 2$. In Figure 6 we display a typical vorticity configuration, where (-) corresponds to the center of a vortex blob with a negative circulation and (+) with a positive circularion. This figure was obtained with $k=0.2$, $h=0.2$, $u_{\max}=0.2$, $R=10^4$, at $t=6.0$.

7. CONCLUSION

We have presented a new elliptic-vortex model for the Navier–Stokes equations, which greatly improves the convergence and the accuracy of the vortex model for boundary-layer flows. Numerical results indicate that the new model, which includes the new boundary algorithm and the new outflow condition, is very effective for calculating flat plate flows. The behavior of the boundary layer at Reynolds numbers

where instability is expected may be seen by this new model. We hope that this method will be applied to other kinds of boundary-flow problems. A generalization of the elliptic-vortex model to three-dimensional flow problems is being considered.

ACKNOWLEDGMENTS

I am grateful to Professor Alexandre J. Chorin for his kind help and for many helpful discussions and comments. I also extend thanks to Dr. A. Y. Cheer for her useful comments on my paper.

This work was carried out while the author was visiting the University of California, Berkeley.

REFERENCES

1. W. R. ASHURST, *in* "Turbulent Shear Flow, I" (F. Durst *et al.*, Eds.), p. 402, Springer-Verlag, Berlin, 1979.
2. T. BEALE AND A. MAJDA, Vortex methods: Convergence in three dimensions, *Math. Comp.*, to appear.
3. A. Y. CHEER, A Study of Incompressible 2-*D* Vortex Flow Past Smooth Surfaces, Lawrence Berkeley Laboratory Report LBL-9950, July 1979, Lawrence, California.
4. A. J. CHORIN, *J. Fluid Mech.* **57** (1973), 785.
5. A. J. CHORIN, *J. Comput. Phys.* **27** (1978), 428.
6. A. J. CHORIN, *SIAM. Sci. Stat. Comput.* **1** (1980), 1.
7. A. J. CHORIN, T. J. R. HUGHES, M. T. MCCRACKEM, AND J. E. MARSDEN, *Comm. Pure Appl. Math.* **31** (1978), 205.
8. A. J. CHORIN AND J. E. MARSDEN, A Mathematical Introduction to Fluid Mechanics, Springer-Verlag, New York, 1979.
9. O. HALD, *SIAM J. Numer. Anal.* **16** (1979), 726.
10. G. W. HEDSTROM AND A. ORTENHELD, *J. Comput. Phys.* **37** (1980), 399.
11. J. JORDINSON, *J. Fluid Mech.* **43** (1970), 801.
12. A. LEONARD, *J. Comput. Phys.* **37** (1980), 289.
13. C. C. LIN, The Theory of Hydrodynamic Stability, Cambridge Univ. Press, London, 1961.
14. A. SHESTAKOV, *in* "Proceeding of 5th International Conference on Numerical Methods in Fluid Dynamics," Springer, New York, 1977.
15. F. M. WHITE, Fluid Mechanics, McGraw–Hill, New York, 1979.